



This open access document is posted as a preprint in the Beilstein Archives at <https://doi.org/10.3762/bxiv.2020.131.v1> and is considered to be an early communication for feedback before peer review. Before citing this document, please check if a final, peer-reviewed version has been published.

This document is not formatted, has not undergone copyediting or typesetting, and may contain errors, unsubstantiated scientific claims or preliminary data.

**Preprint Title** Synthesis of 1-Indolyl-3,5,8-Substituted  $\gamma$ -Carbolines: One Pot Metal-Solvent Free Protocol and Biological Evaluation

**Authors** Premansh Dudhe, Mena A. Krishnan, Kratika Yadav, Diptendu Roy, Krishnan Venkatasubbaiah, Biswarup Pathak and Venkatesh Chelvam

**Publication Date** 19 Nov 2020

**Article Type** Letter

**Supporting Information File 1** Supporting Information.docx; 16.0 MB

**ORCID<sup>®</sup> iDs** Premansh Dudhe - <https://orcid.org/0000-0001-9451-1343>;  
Venkatesh Chelvam - <https://orcid.org/0000-0001-9593-3759>

# Synthesis of 1-Indolyl-3,5,8-Substituted $\gamma$ -Carbolines: One Pot Metal-Solvent Free Protocol and Biological Evaluation

Premansh Dudhe,<sup>a</sup> Mena Asha Krishnan,<sup>b</sup> Kratika Yadav,<sup>b</sup> Diptendu Roy,<sup>a</sup> Krishnan Venkatasubbaiah,<sup>c</sup> Biswarup Pathak,<sup>a</sup> Venkatesh Chelvam<sup>\*,a,b</sup>

**Abstract:** 1,5-Disubstituted indole-2-carboxaldehyde derivatives (**1a–h**) and glycine alkyl esters (**2a–c**) are shown to undergo a novel cascade imination-heterocyclisation in the presence of organic base DIPEA to provide 1-indolyl 3,5,8-substituted  $\gamma$ -carbolines (**3aa–ea**) in good yields. The  $\gamma$ -carbolines are fluorescent and exhibit anticancer activities against cervical, lung, breast, skin and kidney cancers.

**Keywords:**  $\gamma$ -Carboline; cascade reaction; cytotoxicity; cell uptake; density functional theory; fluorescence.

## 1. Introduction

Carbolines are privileged aza-heterocycles found in the core of several natural, synthetic compounds and known for their biological applications. Among the four different isomers, 9*H*-pyrido[3,4-*b*]indole ( $\beta$ -carboline) is the most naturally abundant, for instance, harmine alkaloids, the well-known selective inhibitor of monoamine oxidase-A (MAO-A).<sup>1</sup> On the contrary, 5*H*-pyrido[4,3-*b*]indole ( $\gamma$ -carboline) are comparatively less studied, although these heterocycles have shown promising biological activities in clinical and preclinical studies (Figure 1).<sup>2</sup> The pyrimidine- $\gamma$ -carboline alkaloid ingenine B (isolated from an Indonesian sponge) exhibited pronounced cytotoxicity against murine lymphoma.<sup>3</sup>

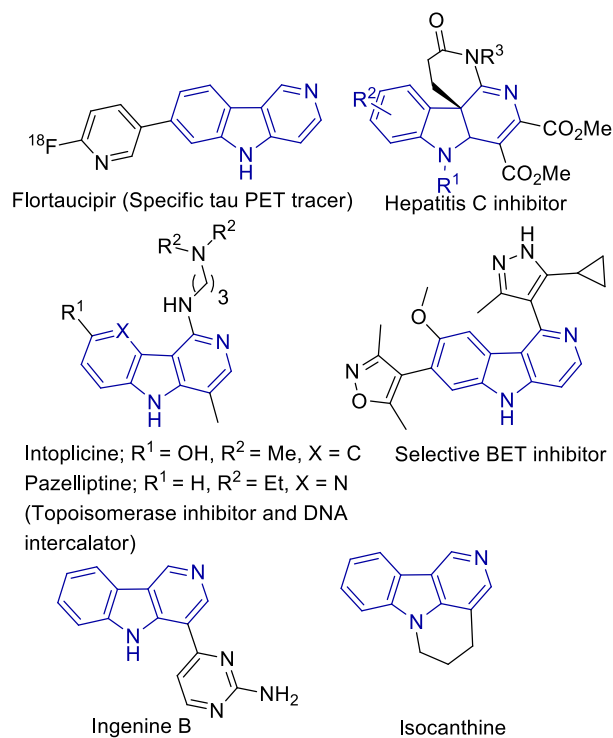


**Figure 1.** Selected examples of compounds containing  $\gamma$ -carboline core

Several isocanthine analogues are effective against cervical cancer (HeLa cells).<sup>4</sup> Moreover,  $\gamma$ -carbolines are known for their well-established DNA intercalating<sup>5</sup> and anti-alzheimer<sup>6</sup> properties. A cascade or domino reaction is an interesting research domain to design efficient one-step transformation for complex molecule synthesis.<sup>7</sup> Employing these domino reactions to simplify cumbersome industrial processes can afford complex pharmaceutical products economical and their synthesis environmentally benign.<sup>8</sup> Easy workup procedures and single step purification reduces the efforts in synthesis of complex molecular architectures. Therefore, cascade reactions are very important in synthetic organic chemistry, even with their moderate yields.<sup>9</sup> Recently, such reactions have claimed their much deserving place in drug designing and natural product synthesis.<sup>10</sup>

In the literature, only a limited number of direct synthetic procedures are available for  $\gamma$ -carbolines till date,<sup>11</sup> and this gives a cutting edge advantage to the newly developed protocol reported herein for the synthesis of this unique heterocyclic scaffold.

The classical Graebe-Ullman synthesis of  $\gamma$ -carbolines, one of the very early protocols in the domain, was based on thermal decomposition of *N*-pyridylbenzotriazoles. Later, the reaction conditions were modified to make this reaction more versatile and operationally simple viz., use of microwave irradiation.<sup>12</sup> Meanwhile, the Fischer indole synthesis was successfully extended towards the synthesis of biological significant tetrahydro- $\gamma$ -carboline derivatives.<sup>13,14</sup> A systematic assessment of above protocols on Graebe-Ullmann and Fischer synthesis reveals i) less product yield ii) limited scope including the use of very specific set of substrates, and iii) involvement of extreme thermal conditions with use of corrosive reagents. Much later, Larock and co-workers developed Pd/Cu catalyzed imino-annulation of internal alkynes,<sup>15</sup> which paved the way for transition-metal catalysed cyclization as an easy access to these scaffolds. Notably, gold catalysed tandem cycloisomerization/Pictet–Spengler cyclisation of 2-(4-aminobut-1-yn-1-yl)aniline,<sup>16</sup> Ru and Rh catalysed [2+2+2] cycloadditions of yne-ynamides,<sup>17</sup> and Pd catalysed tandem coupling-cyclisation<sup>18</sup> are significant works in the area. However, the use of toxic and expensive metal catalysts has limited their development as environment friendly synthetic protocols. More recently, acid catalysed cyclisation of  $\alpha$ -indol-2-yl methyl TosMIC derivatives to synthesize heterocycles<sup>19</sup> has been thoroughly studied, including synthesis of carboline alkaloid Ingenine B.<sup>20</sup> Iodine catalysed [3+3] cycloaddition of indolyl alcohol to enaminones<sup>21</sup> and thiourea catalysed iso-Pictet–Spengler reaction of isotryptamine with aldehydes,<sup>22</sup> are some noteworthy contributions in the field.

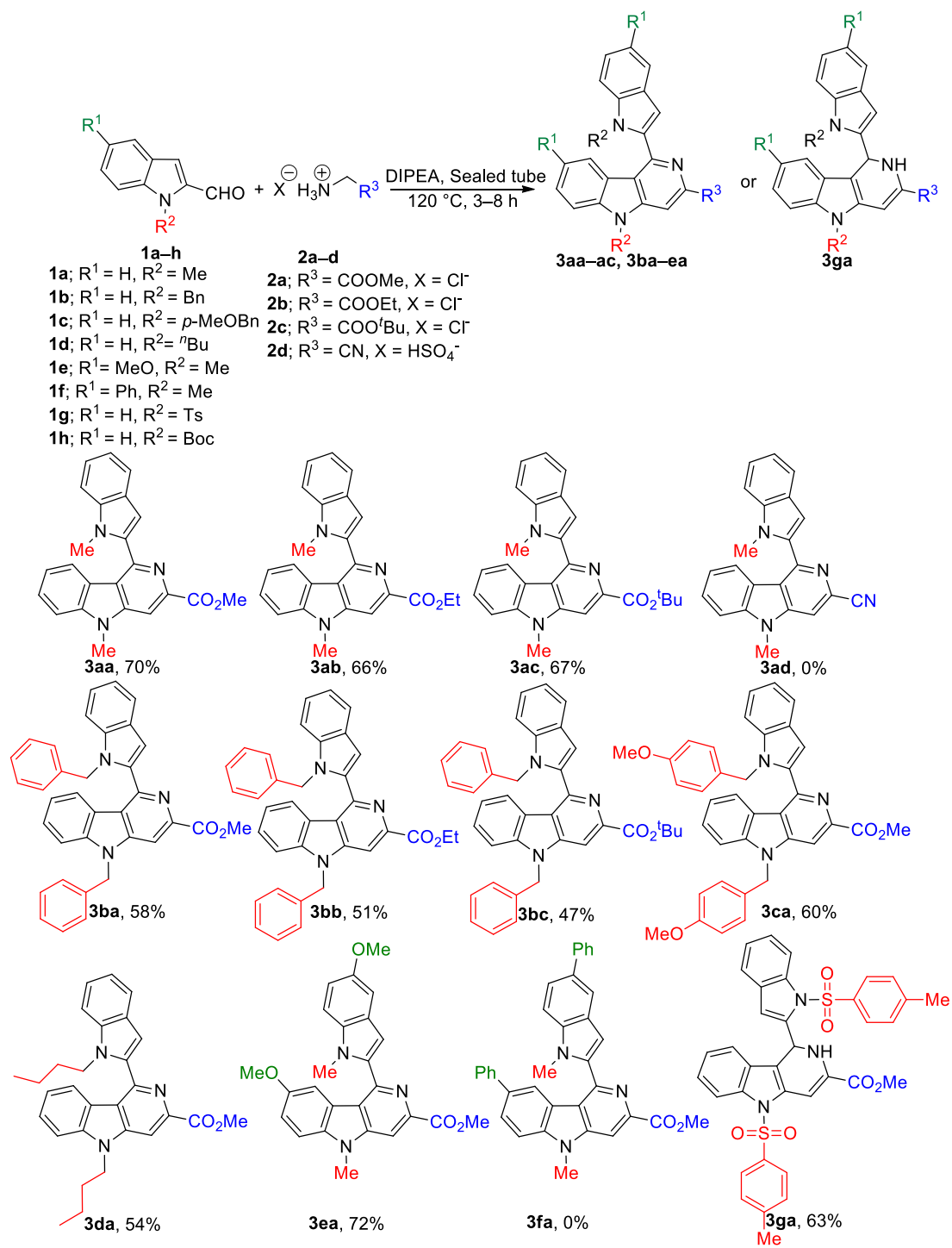
## 2. Results and Discussion

### 2.1. Optimisation of reaction conditions and chemical synthesis

The base catalysed imination of aromatic aldehydes is a useful method in organic synthesis to synthesize a variety of heterocyclic building blocks.<sup>23</sup> Among all the reported iminoesters, alkyl-*N*-arylidene-glycinates have attracted much attention in recent years. For instance, metal catalysed asymmetric [3+2] cycloaddition of ethyl *N*-benzylidene-glycinate with electron-deficient alkenes has been reported to yield substituted pyrrolidines.<sup>24</sup>

Recently, we reported synthesis of substituted pyrrole-2-aldehydes to 5-azaindole transformation during a base catalysed imination reaction.<sup>25</sup> However, we envisioned that our methodology may be strategically applied towards synthesis of substituted  $\gamma$ -carbolines as C-3 nucleophilic attack is more pronounced in indoles than pyrroles. Herein, we report an interesting observation for conversion of substituted indole-2-aldehydes (**1**) to 1-indolyl-3,5,8-substituted  $\gamma$ -carbolines (**3**) by a cascade imination-heterocyclisation pathway when treated with glycine methyl ester hydrochloride salt in the presence of a base. Earlier in the literature it was reported that 1*H*-indole-2-carbaldehyde derivatives underwent condensation with *N*-arylidene-glycinate to form pyrimidoindole derivatives.<sup>26</sup> Whereas when 1-methyl-1*H*-indole-2-carbaldehyde (**1a**) and glycine methyl ester hydrochloride salt (**2a**) were reacted in the presence of DIPEA (Hunig's base) at room temperature in non-polar solvent such as toluene only marginal amounts of corresponding imine was observed, which could not be isolated (Table 1; entry 1). When the reaction mixture was further heated to reflux for 16 h, traces of 1-indolyl 3,5,8-substituted  $\gamma$ -carboline (**3aa**) was formed but insufficient for complete characterization. With the intention of improving the yield of **3aa**, we screened various solvents, non-nucleophilic organic bases such as

triethylamine and DBU, and a number of inorganic bases like  $K_2CO_3$ ,  $Cs_2CO_3$  and NaH (Table 1; entries 2–6).



**Scheme 1.** Series of 1-indolyl-3,5,8-substituted  $\gamma$ -carboline (**3aa–ac**, **3ba–ea**) and 1-indolyl-1,2-dihydro-3,5-substituted  $\gamma$ -carboline (**3ga**) derivatives

After a systematic scrutiny of a number of reaction conditions, it was found that when a mixture of 1-methyl-1*H*-indole-2-carbaldehyde, **1a**, (2.0 equiv.), glycine methyl ester HCl salt **2a**, (1.0 equiv.) and DIPEA (3.5 equiv.) was heated neat at 120 °C in a sealed tube for 6 h, we were delighted to obtain **3aa** in 70% yield (Table 1; entry 7), which was further characterized by various spectroscopic techniques.

Entry	Base (3.5 equiv.)	Solvent	Temp.	Yield
1	DIPEA	Toluene <sup>a</sup>	RT to reflux	Trace
2	Et <sub>3</sub> N	Toluene <sup>a</sup>	RT to reflux	No product
3	DBU	Toluene <sup>a</sup>	RT to reflux	Trace
4	K <sub>2</sub> CO <sub>3</sub>	Et <sub>2</sub> O <sup>a</sup>	RT to reflux	No product
5	Cs <sub>2</sub> CO <sub>3</sub>	DMF <sup>a</sup>	RT to reflux	No product
6	NaH	THF <sup>a</sup>	RT to reflux	No product
7	DIPEA <sup>b</sup>	---	120 °C	70%

**Table 1.** Optimization of reaction conditions: <sup>a</sup>Reactions were monitored by TLC for 3 h at room temperature followed by reflux for 16 h in the appropriate solvent; <sup>b</sup>Solvent-free reaction carried out in a 25 mL borosilicate sealed tube in a preheated oil bath in normal atmosphere at 120 °C.

With the preliminary success at our hand, the reaction was found to be equally effective with various glycine alkyl ester HCl salts (**2a–2c**) but failed to result in the formation of 1-

indolyl-3-cyano-5-methyl  $\gamma$ -carboline derivative (**3ad**) when 2-aminoacetonitrile (**2d**) was utilized as the condensation component. A range of 1,5-substituted indole-2-carboxaldehyde derivatives (**1a–h**) were synthesized (see supporting information) to evaluate the scope of the reaction. It was observed that indole-2-aldehyde derivatives with electron donating 1-substituent on the indole ring system (**1a–1e**) were transformed in moderate to good yields into their corresponding  $\gamma$ -carboline derivatives (**3aa–ac**, **3ba–ea**) due to enhanced C-3 nucleophilicity of indole nucleus. The formation of  $\gamma$ -carboline was confirmed unequivocally by single crystal X-ray diffraction analysis of **3ac** (Figure 2).

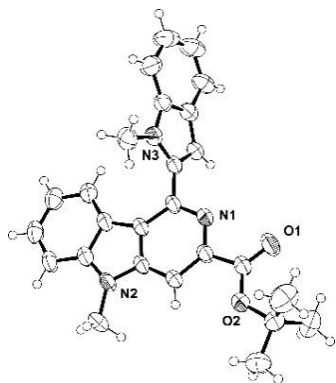


**Figure 2.** Single crystal XRD structure of **3ac** (CCDC: 1897787)

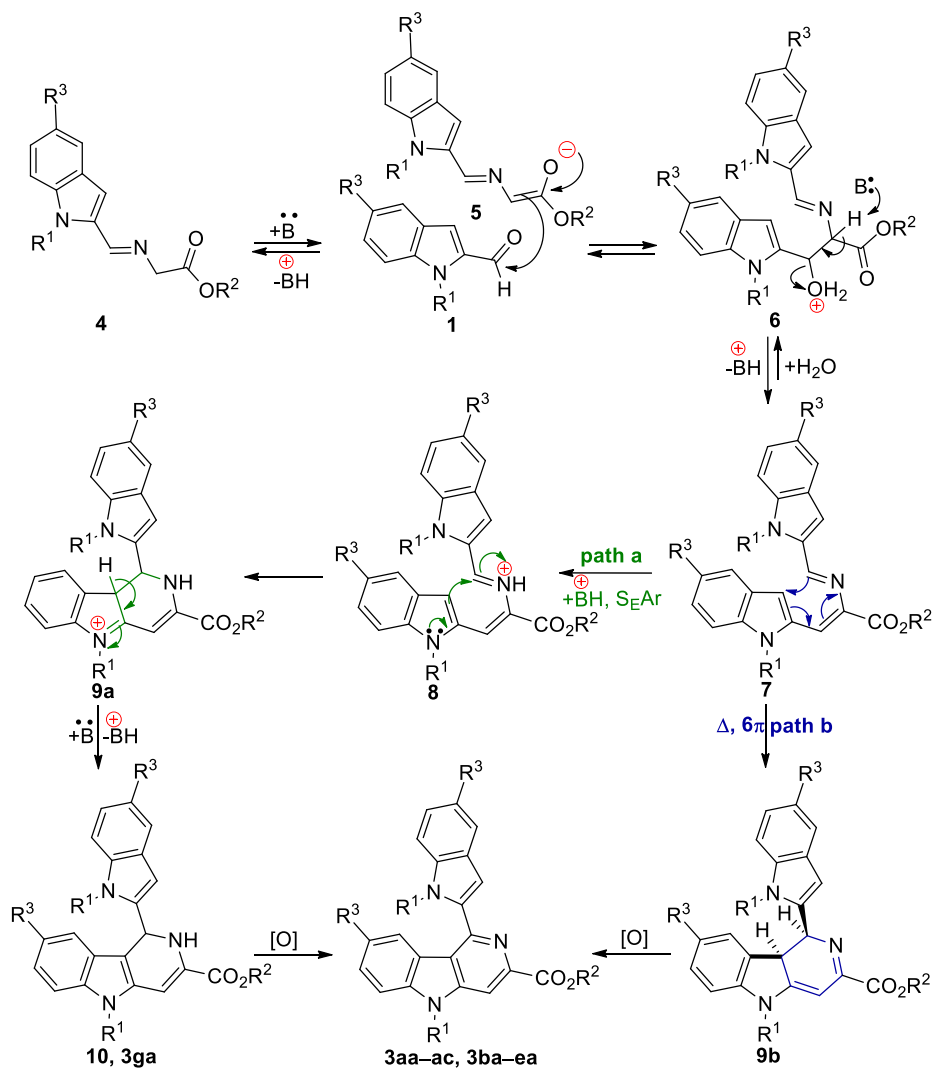
Presence of both 1,5-substituents in the indole-2-carbaldehyde substrates such as **1e** (5-methoxy-1-methyl-1*H*-indole-2-carbaldehyde) and **1f** (1-methyl-5-phenyl-1*H*-indole-2-carbaldehyde) influence the outcome of the heterocyclization reaction in different ways. For eg., **1e** was successfully transformed into 1-indolyl-3-carbomethoxy-5-methyl-8-methoxy  $\gamma$ -carboline **3ea** in 72% yield whereas, **1f** remain unreacted under optimized reaction condition and didn't yield the expected 5-methyl-1-(1-methyl-5-phenyl-1*H*-indol-2-yl)-3-carbomethoxy-8-

phenyl  $\gamma$ -carboline derivative (**3fa**), perhaps due to severe steric hindrance between 1-(1-methyl-5-phenyl-1*H*-indol-2-yl) and 8-phenyl substituents in the  $\gamma$ -carboline framework of **3fa**.

Mild electron withdrawing 1-substituent such as *N*-tosyl in 1-tosyl-1*H*-indole-2-carbaldehyde (**1g**) did not affect the reaction course and the substrate was smoothly transformed to corresponding 1-indolyl-3,5-substituted 1,2-dihydro- $\gamma$ -carboline derivative **3ga** instead of completely aromatized  $\gamma$ -carboline when heated at 120 °C with glycine methyl ester hydrochloride and DIPEA for 8 h in a sealed tube. However, strong electron withdrawing 1-substituent such as *N*-Boc group in 1-*tert*-butyloxycarbonyl-1*H*-indole-2-carbaldehyde (**1h**), impeded the conversion to  $\gamma$ -carboline (**3ha**) (structure not shown) due to drastic decrease in nucleophilicity at 3-position of **1h**.

## 2.2. Plausible mechanism for the formation of $\gamma$ -carbolines

The probable mechanistic explanation (Scheme 2) for the formation of  $\gamma$ -carboline derivatives (**3aa–ac**, **3ba–ea**) involves the initial formation of *trans*-iminoester **4** from *N*-protected indole-2-carboxaldehyde (**1a–e**, **1g**) and glycine alkyl esters (**2a–c**). The Hunigs base,



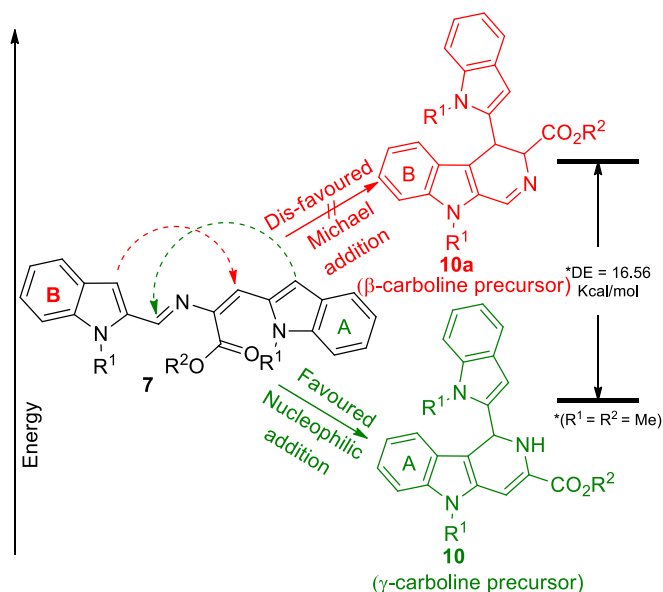
**Scheme 2.** Plausible mechanism for the formation of 1-indolyl-3,5,8-substituted  $\gamma$ -carbolines **3aa-ac**, **3ba-ea** and 1,2-dihydro  $\gamma$ -carboline derivative **3ga**

DIPEA, helps abstract active methylene proton from iminoester **4** to generate enolate ion **5**, which undergoes nucleophilic addition with another molecule of aldehyde **1** to furnish iminoalcohol intermediate **6**. The iminoalcohol **6** undergoes dehydration under the reaction condition to give iminoenamine intermediate **7** which play decisive role in determining ring closure *via* either path a or path b.

In path a, protonation of imine nitrogen by conjugate acid (+BH) drives the reaction in forward direction by electrophilic aromatic substitution at 3-position of the indole unit to form carbon-carbon bond in the intermediate **9a**. Further, proton abstraction by base gives 1-indolyl-3,5-substituted 1,2-dihydro- $\gamma$ -carboline intermediate **10** or **3ga**. In path b, intermediate **7** would undergo thermal 6- $\pi$  electrocyclic reaction of a conjugated triene system to form 1-indolyl-3,5-substituted 1,2-dihydro- $\gamma$ -carboline **9b**. *In situ* oxidation of **9b** or **10**, probably from the dissolved oxygen present in the reaction mixture, leads to the formation of 1-indolyl-3,5,8-substituted  $\gamma$ -carbolines (**3aa-ac**, **3ba-ea**). We were successfully able to isolate and characterize 1,2-dihydro  $\gamma$ -carboline derivative **3ga**, which again verifies the proposed mechanism.

### 2.3. Density functional theory explanation for the formation of $\gamma$ -carbolines

During the formation of carbolines, the substrates, **1a-e**, **1g** were exclusively transformed to  $\gamma$ -carbolines or 1,2-dihydro- $\gamma$ -carboline (**10**) and no traces of  $\beta$ -carboline regioisomers (**10a**) were observed which proves that the heterocyclization reaction is highly regioselective (Scheme 3). The exclusive formation of  $\gamma$ -carboline regioisomer is explained by proposing an intermediate **7** before heterocyclization reaction takes place. Indole ring A predominantly participate in nucleophilic addition on the intermediate **7** over Michael addition of indole ring B. Density functional theoretical calculations<sup>27</sup> (see supporting information) also support that nucleophilic addition is favoured by 16.56 Kcal/mol over Michael addition, between the formation of  $\gamma$ - and  $\beta$ -carbolines **10** and **10a**. This indicates that  $\gamma$ -regioisomer **10** is thermodynamically stable over  $\beta$ -regioisomer **10a** (Scheme 3).



**Scheme 3.** DFT relative energy calculation for the formation of  $\gamma$ -carboline (**10**) over  $\beta$ -carboline (**10a**) regioisomer using B3LYP/6-311++G\*\* level of theory

#### 2.4. Optical properties of $\gamma$ -carboline

Interestingly, the  $\gamma$ -carboline derivatives were found to be highly fluorescent under UV illumination. A systematic literature survey revealed that the structural armamentarium of carbolines has been widely exploited for the development of organic fluorescent entities, and in general, their UV absorbance ranges between 340 to 380 nm. For deeper insight into the optical properties of novel substituted  $\gamma$ -carbolines, absorption and emission studies were carried out in different organic solvents (Figure 4). The representative  $\gamma$ -carboline derivative *tert*-butyl 5-methyl-1-(1-methyl-1*H*-indol-2-yl)-5*H*-pyrido[4,3-*b*]indole-3-carboxylate (**3ac**) revealed almost identical absorption features in different solvents irrespective of their polarity. Highest absorption maximum ( $\lambda_{\text{max}}$ ) was observed at 230 nm for **3ac** in DMSO.

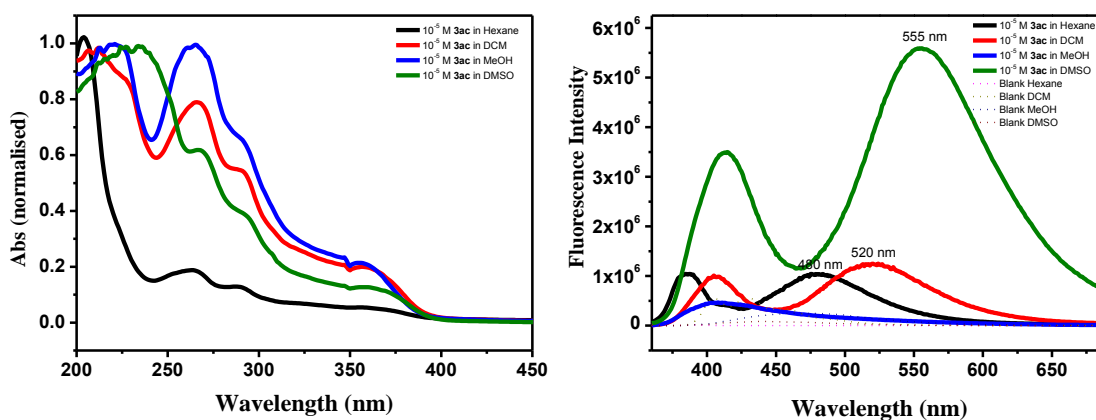


**Figure 4.** UV-vis absorption (left side) and emission (right side) spectra of **3ac** measured in different solvents

The fluorescence studies were carried out for **3ac** in four different solvents reveal that emission maxima shifts bathochromically by almost 40 nm upon changing the solvent polarity, for instance from non-polar hexane to moderately polar dichloromethane and then highly polar DMSO (Table 2; Figure 4). The fluorescence quenching of **3ac** in polar-protic solvent, methanol, can be attributed to the ultrafast solute-solvent intermolecular photo-induced electron transfer facilitated by hydrogen bonding interactions.<sup>28</sup>

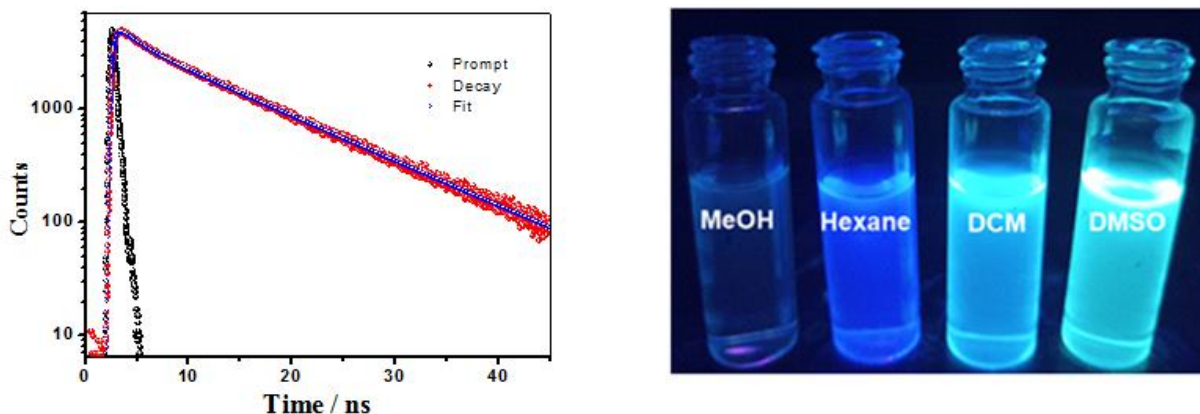


**Figure 5.** Fluorescence decay profile of **3ac** in DMSO (left side;  $\lambda_{\text{exc}}$  360 nm) and  $10^{-5}$  M solutions of compound **3ac** in four different solvents under UV chamber (right side)

Fluorescence life-times were measured by time-correlated single-photon counting (TCSPC) experiments. Generally, longer fluorescence life-times are correlated with higher quantum yields and good imaging contrast. To our surprise, synthesized  $\gamma$ -carboline **3ac** was found to be highly fluorescent in DMSO and DCM with an average fluorescence life-time of 8.35 nanoseconds (ns) and 4.73 ns, respectively (Table 2; Figure 5).

Solvent	$\lambda_{\text{abs}}$ (nm)	$\epsilon$ ( $10^3 \text{ M}^{-1} \text{ cm}^{-1}$ )	$\lambda_{\text{em}}$ (nm)	$\tau$ (ns)
Hexane	204, 262, 290, 355	0.78	386, 480	1.90
DCM	210, 266, 290, 356	1.01	405, 520	4.73
MeOH	220, 265, 290, 355	2.05	407, 422	0.99
DMSO	230, 266, 290, 357	1.67	413, 555	8.35

**Table 2.** Optical data for  $\gamma$ -carboline **3ac**

### 2.5. Biological evaluation of $\gamma$ -carbolines as anticancer agents

A panel of carboline derivatives **3ac**, **3bc**, **3ca**, and **3ga** were also screened for their cytotoxicity against various cancer lines (Figure 6, Table 3 and Figure S3, Supporting information) such as MCF-7 (breast cancer), A431 (skin cancer), A549 (lung cancer), HEK293 (human embryonic kidney cells), HeLa (cervical cancer), and macrophage or immune cell line (RAW 264.7).

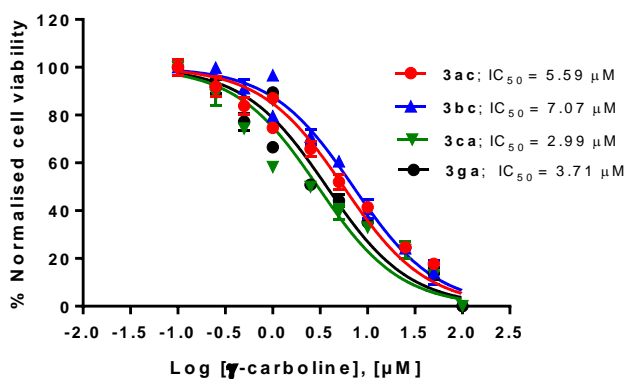


**Figure 6.** Dose vs response curve of  $\gamma$ -carbolines **3ac**, **3bc**, **3ca**, **3ga** in breast cancer cell line, MCF7

$\gamma$ -Carboline	IC <sub>50</sub> in Cancer cell lines ( $\mu$ M)				
	MCF7	A431	A549	HEK293	HeLa
<b>3ac</b>	5.59	4.89	4.76	2.29	4.89
<b>3bc</b>	7.07	9.18	5.53	7.14	8.15
<b>3ca</b>	2.99	4.47	5.27	6.73	1.30
<b>3ga</b>	3.71	3.57	5.05	4.98	1.07

**Table 3.** IC<sub>50</sub> values of  $\gamma$ -carbolines **3ac**, **3bc**, **3ca**, **3ga** in various cancer cell lines

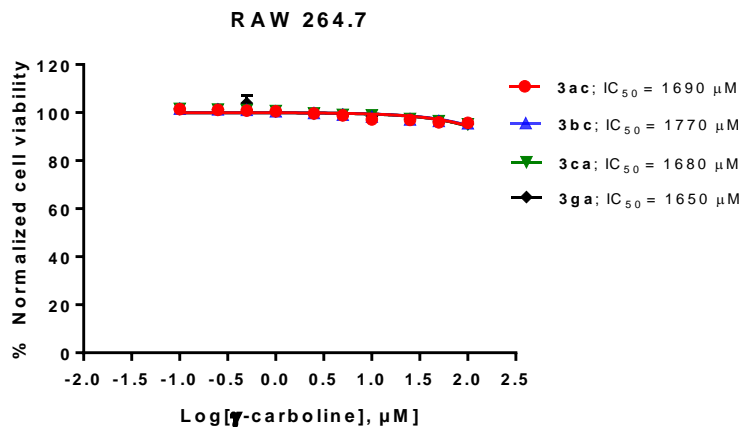


**Figure 7.** Dose vs response curve of  $\gamma$ -carbolines **3ac**, **3bc**, **3ca**, **3ga** in macrophage cell line, RAW264.7

Cancer cells were treated with an increasing concentration of carboline derivatives **3ac**, **3bc**, **3ca** and **3ga** (0.1  $\mu$ M, 0.25  $\mu$ M, 0.5  $\mu$ M, 1  $\mu$ M, 2.5  $\mu$ M, 5  $\mu$ M, 10  $\mu$ M, 25  $\mu$ M, 50  $\mu$ M, 100  $\mu$ M) and incubated for 48 h. Half-maximal inhibitory studies show that  $\gamma$ -carbolines are highly toxic to cancer cells in micromolar concentrations whereas it is non-cytotoxic (Figure 7) to human macrophages or immune cells.

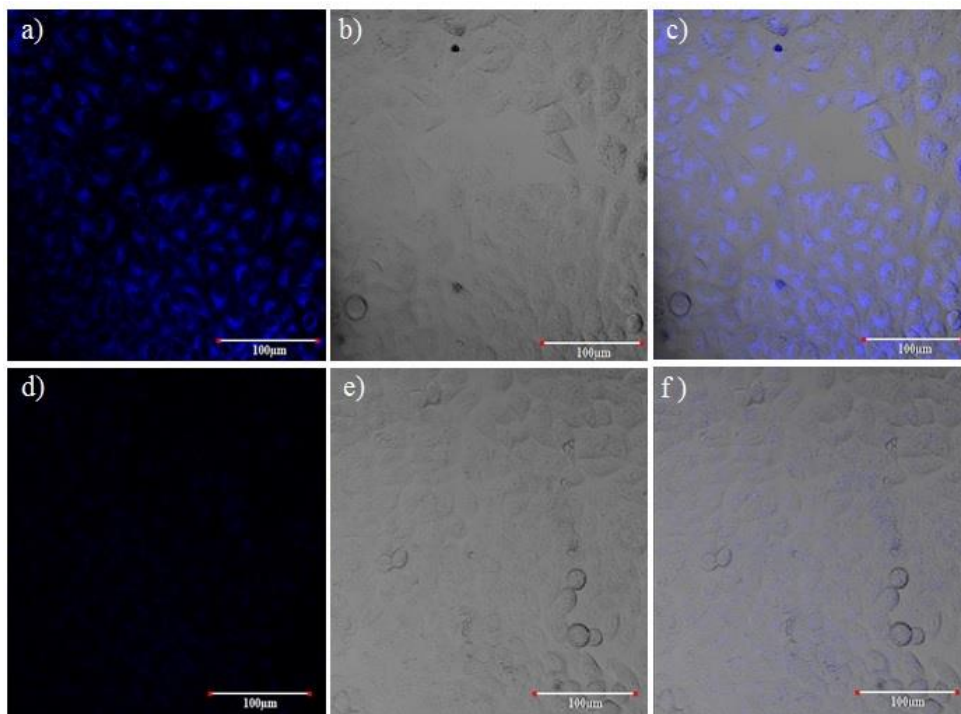


**Figure 8.** Laser scanning confocal microscopy studies ( $\lambda_{\text{ex}} = 405 \text{ nm}$ ; collection range= 420–470 nm) for uptake of **3ac** in HeLa cells; a) Confocal fluorescent image of HeLa cells after 3 h incubation with 10  $\mu\text{M}$  concentration of **3ac** (20X magnification, 2X zoom); b) DIC image of HeLa cells; c) Overlay of (a) and (b) indicating distribution of **3ac** in cytoplasm with distinct cell nucleus; d) Confocal image of HeLa cells after 3 h incubation with 100 nM concentration of **3ac** (20X magnification, 2X zoom); e) DIC image of HeLa cells; f) Overlay of (d) and (e) showing nominal uptake of **3ac** in cytoplasm.

At last, to evaluate cell uptake of the novel  $\gamma$ -carboline for fluorescence imaging, live-cell imaging experiments were performed. HeLa cells were incubated with **3ac** (10 nM, 100 nM, 1  $\mu\text{M}$ , 10  $\mu\text{M}$ , and 100  $\mu\text{M}$ ) and the cellular uptake were examined using confocal microscopy ( $\lambda_{\text{ex}} = 405 \text{ nm}$ ;  $\lambda_{\text{em}} = 420\text{--}470 \text{ nm}$ ). **3ac** show excellent cytosolic uptake in cancer cells while

incubation with 10  $\mu\text{M}$  concentration, whereas nominal uptake was observed for 100 nM concentration (Figure 8).

### **3. Conclusion**

In summary, we have developed an operationally simple one-pot synthetic protocol for synthesis of highly substituted  $\gamma$ -carboline derivatives. The metal- and solvent-free protocol provides direct access to complex molecular structure in good yield from inexpensive substrates. Optical and biological evaluations carried out for representative  $\gamma$ -carbolines reveal promising photophysical and anticancer properties of the core framework for developing novel theranostic applications to diagnose and treat cancer in future.

### **4. Experimental section**

#### *4.1. Synthesis*

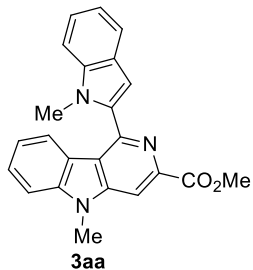
##### *4.1.1. General methods and materials*

All reactions were carried out in oven dried glasswares with magnetic stirring. Starting materials and other reagents were obtained from commercial supplier and used without further purification. NMR spectra were recorded on Avance III 400 Ascend Bruker.  $\text{CDCl}_3$  and  $\text{D}_2\text{O}$  were used as NMR solvents. Chemical shifts ( $\delta$ ) reported as part per million (ppm) and TMS was used as internal reference. High resolution mass spectra were recorded through Bruker Daltonik High Performance LC MS (Electrospray Ionization Quadrupole time-of-flight) spectrometer. X-ray structure analysis was carried out at Single crystal X-ray diffractometer Bruker KAPPA APEXII. Melting points (m.p.) are uncorrected and were measured on Veego melting point apparatus (Capillary method). Analytical thin layer chromatography (TLC) was carried out on

silica gel plates (silica gel 60 F254 aluminium supported plates); the visualization was accomplished with an UV lamp (254 nm and 365 nm) and using chemical staining with Brady's reagent, KMnO<sub>4</sub>, ninhydrin, iodine, and bromocresol. Column chromatography was performed using silica gel (100–200 mesh or 230–400 mesh) and neutral alumina (175 mesh). DMF, DCM, DMA, Toluene, and Acetonitrile were dried using CaH<sub>2</sub> and distilled over flame-dried 4Å molecular sieves. THF and Et<sub>2</sub>O were dried over Na/benzophenone and stored over flame-dried 4Å molecular sieves under inert atmosphere prior to use. Organic bases including DIPEA, Et<sub>3</sub>N, and DBU were stored over anhydrous KOH pellets.

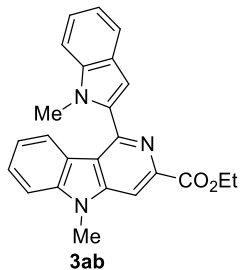
*4.2.2. General procedure for the synthesis of 1-indolyl-3,5,8-substituted  $\gamma$ -carboline (3aa–ac, 3ba–ea) and 1-indolyl-1,2-dihydro-3,5-substituted  $\gamma$ -carboline (3ga) derivatives*

A mixture of *N*-substituted indole-2-aldehyde (**1a–h**, 2.0 mmol), glycine alkyl ester hydrochloride (**2a–c**, 1.0 mmol) and DIPEA (3.5 mmol) was heated in a sealed tube for 3–8 h at 120 °C. After the completion of reaction as evident by TLC, the reaction mixture was diluted with dichloromethane (CH<sub>2</sub>Cl<sub>2</sub>, 10 mL) and washed with cold brine (10 mL). The aqueous layer was again extracted with CH<sub>2</sub>Cl<sub>2</sub> (3 × 10 mL). Organic layers were pooled and dried over anhydrous Na<sub>2</sub>SO<sub>4</sub>, filtered, concentrated under reduced pressure, and purified over neutral alumina gel (175 mesh) column chromatography, using a mixture of ethyl acetate and hexane as eluent to afford products **3aa–ac**, **3ba–ea** and **3ga**.



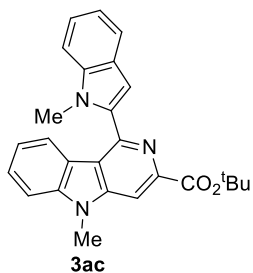
*Methyl 5-methyl-1-(1-methyl-1H-indol-2-yl)-5H-pyrido[4,3-b]indole-3-*

*carboxylate (3aa)*. According to the general procedure mentioned above, **1a** (0.100 g, 0.62 mmol), **2a** (39 mg, 0.31 mmol) and DIPEA (0.190 mL, 1.09 mmol) were heated in a sealed tube at 120 °C for 6 h. After workup, crude mixture was purified through alumina (neutral, 175 mesh) column chromatography using hexane-EtOAc (80:20) as eluent; Yield 70% (80 mg); Yellow solid; m.p. = 210–212 °C;  $R_f$  0.35 (2:1 hexane-EtOAc); IR (KBr) 3055 (=C–H), 2956–2854 (C–H), 1734 (C=O), 1687–1534 (C=C), 1407–1376 (C–H bend), 782 (=C–H bend)  $\text{cm}^{-1}$ ;  $^1\text{H}$  NMR (400 MHz,  $\text{CDCl}_3$ )  $\delta$  8.31 (s, 1H), 7.82 (d,  $J = 8.0$  Hz, 1H), 7.74 (d,  $J = 8.0$  Hz, 1H), 7.56 (dd,  $J = 8.0, 7.3$  Hz, 1H), 7.51 (d,  $J = 8.3$  Hz, 1H), 7.45 (d,  $J = 8.3$  Hz, 1H), 7.33 (dd,  $J = 8.0, 7.8$  Hz, 1H), 7.19 (dd,  $J = 7.5, 7.5$  Hz, 1H), 7.15 (dd,  $J = 7.6, 7.5$  Hz, 1H), 6.99 (s, 1H), 4.05 (s, 3H), 4.00 (s, 3H), 3.75 (s, 3H);  $^{13}\text{C}$  NMR (100 MHz,  $\text{CDCl}_3$ )  $\delta$  166.9, 146.3, 145.8, 142.9, 142.2, 138.3, 137.6, 128.1, 127.9, 123.1, 122.4, 121.3, 121.2, 121.1, 120.8, 119.8, 109.8, 109.1, 105.7, 104.3, 53.0, 31.0, 29.6; HRMS (ESI) calcd for  $[\text{C}_{23}\text{H}_{19}\text{N}_3\text{O}_2+\text{H}^+]$  370.1550, found 370.1515.



*Ethyl 5-methyl-1-(1-methyl-1H-indol-2-yl)-5H-pyrido[4,3-b]indole-3-*

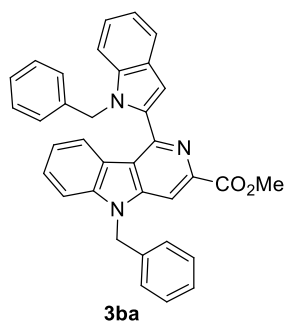
*carboxylate (3ab)*. According to the general procedure mentioned above, **1a** (0.100 g, 0.62 mmol), **2b** (43 mg, 0.31 mmol) and DIPEA (0.190 mL, 1.09 mmol) were heated in a sealed tube at 120 °C for 6 h. After workup, crude mixture was purified through alumina (neutral, 175 mesh) column chromatography using hexane-EtOAc (85:15) as eluent; Yield 66% (78 mg); Yellow solid; m.p. = 175–177 °C;  $R_f$  0.40 (2:1 hexane-EtOAc); IR (KBr) 3058 (=C–H), 2988–2851 (C–H), 1735 (C=O), 1704–1536 (C=C), 1409–1375 (C–H bend), 780 (=C–H bend)  $\text{cm}^{-1}$ ;  $^1\text{H}$  NMR (400 MHz,  $\text{CDCl}_3$ )  $\delta$  8.27 (s, 1H), 7.89 (d,  $J$  = 8.0 Hz, 1H), 7.73 (d,  $J$  = 7.8 Hz, 1H), 7.56 (dd,  $J$  = 7.8, 7.3 Hz, 1H), 7.50 (d,  $J$  = 8.0 Hz, 1H), 7.46 (d,  $J$  = 8.0 Hz, 1H), 7.33 (dd,  $J$  = 7.8, 7.8 Hz, 1H), 7.19 (m, 2H), 7.01 (s, 1H), 4.53 (q,  $J$  = 7.0 Hz, 2H), 3.99 (s, 3H), 3.79 (s, 3H), 1.48 (t,  $J$  = 7.0 Hz, 3H);  $^{13}\text{C}$  NMR (100 MHz,  $\text{CDCl}_3$ )  $\delta$  166.3, 146.3, 145.9, 143.2, 142.2, 138.3, 137.6, 128.0, 127.8, 123.1, 122.4, 121.2, 121.1, 120.9, 120.8, 119.8, 109.8, 109.1, 105.5, 104.4, 61.9, 31.1, 29.5, 14.5; HRMS (ESI) calcd for  $[\text{C}_{24}\text{H}_{21}\text{N}_3\text{O}_2+\text{H}^+]$  384.1707, found 384.1672.



*Tert-butyl 5-methyl-1-(1-methyl-1H-indol-2-yl)-5H-pyrido[4,3-b]indole-3-*

*carboxylate* (**3ac**). According to the general procedure mentioned above, **1a** (0.100 g, 0.62 mmol), **2c** (52 mg, 0.31 mmol) and DIPEA (0.190 mL, 1.09 mmol) were heated in a sealed tube at 120 °C for 8 h. After workup, crude mixture was purified through alumina (neutral, 175 mesh) column chromatography using hexane-EtOAc (90:10) as eluent; Yield 67% (85 mg); Yellow solid; m.p. = 200–202 °C;  $R_f$  0.60 (2:1 hexane-EtOAc); IR (KBr) 3053 (=C–H), 2972–2852 (C–H), 1729 (C=O), 1686–1532 (C=C), 1412–1365 (C–H bend), 781 (=C–H bend)  $\text{cm}^{-1}$ ;  $^1\text{H}$  NMR (400 MHz,  $\text{CDCl}_3$ )  $\delta$  8.14 (s, 1H), 8.07 (d,  $J$  = 8.0 Hz, 1H), 7.73 (d,  $J$  = 7.8 Hz, 1H), 7.55 (dd,  $J$  = 7.5, 7.5 Hz, 1H), 7.52–7.43 (m, 2H), 7.33 (dd,  $J$  = 8.0, 7.3 Hz, 1H), 7.23–7.11 (m, 2H), 7.06 (s, 1H), 3.97 (s, 3H), 3.88 (s, 3H), 1.69 (s, 9H);  $^{13}\text{C}$  NMR (100 MHz,  $\text{CDCl}_3$ )  $\delta$  165.2, 146.2, 146.1, 144.3, 142.2, 138.4, 137.7, 127.8, 127.7, 123.1, 122.4, 121.2, 120.9\*, 120.3, 119.7, 109.8, 109.0, 104.7, 104.6, 81.9, 31.2, 29.5, 28.3; HRMS (ESI) calcd for  $[\text{C}_{26}\text{H}_{25}\text{N}_3\text{O}_2+\text{H}^+]$  412.2020, found 412.2012.

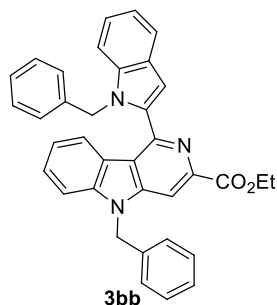
\*Higher intensity carbon



*Methyl 5-benzyl-1-(1-benzyl-1H-indol-2-yl)-5H-pyrido[4,3-b]indole-3-*

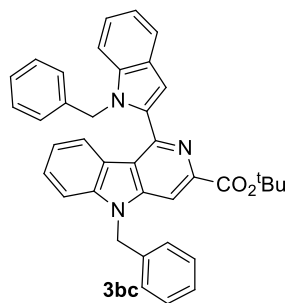
*carboxylate (3ba)*. According to the general procedure mentioned above, **1b** (0.100 gms, 0.42 mmol), **2a** (26 mg, 0.21 mmol) and DIPEA (0.095 mL, 0.74 mmol) were heated in a sealed tube at 120 °C for 6 h. After workup, crude was purified through alumina (neutral, 175 mesh) column chromatography using hexane-EtOAc (85:15) as eluent; Yield 58% (63 mg); Yellow solid; m.p. = 168–170 °C;  $R_f$  0.60 (2:1 hexane-EtOAc); IR (ATR) 3062 (=C–H), 2920–2850 (C–H), 1710 (C=O), 1667–1528 (C=C), 1467–1315 (C–H bend), 787–694 (=C–H bend)  $\text{cm}^{-1}$ ;  $^1\text{H}$  NMR (400 MHz,  $\text{CDCl}_3$ )  $\delta$  8.20 (s, 1H), 8.13 (d,  $J = 8.0$  Hz, 1H), 7.75 (d,  $J = 7.5$  Hz, 1H), 7.48 (dd,  $J = 7.5, 7.3$  Hz, 1H), 7.41 (m, 2H), 7.35–7.23 (m, 4H), 7.20 (d,  $J = 7.5$  Hz, 1H), 7.16 (d,  $J = 8.0$  Hz, 1H), 7.14–7.08 (m, 3H), 6.99–6.89 (m, 5H), 5.67 (s, 2H), 5.60 (s, 2H), 3.98 (s, 3H);  $^{13}\text{C}$  NMR (100 MHz,  $\text{CDCl}_3$ )  $\delta$  166.8, 146.5, 145.8, 142.9, 141.7, 138.3, 138.1, 136.9, 135.6, 129.0, 128.1\*, 128.0, 127.9, 126.7, 126.6, 126.3, 123.3, 122.7, 121.3, 121.13, 121.06, 121.0, 120.0, 110.6, 109.6, 105.7, 105.5, 52.9, 47.7, 46.8; HRMS (ESI) calcd for  $[\text{C}_{35}\text{H}_{27}\text{N}_3\text{O}_2+\text{H}^+]$  522.2176, found 522.2160.

\*Higher intensity carbon



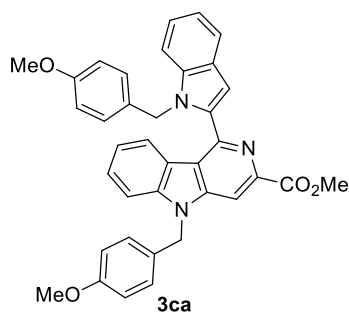
*Ethyl 5-benzyl-1-(1-benzyl-1H-indol-2-yl)-5H-pyrido[4,3-b]indole-3-*

*carboxylate (3bb)*. According to the general procedure mentioned above, **17b** (0.100 g, 0.62 mmol), **2b** (43 mg, 0.31 mmol) and DIPEA (0.190 mL, 1.09 mmol) were heated in a sealed tube at 120 °C for 6 h. After workup, crude was purified through alumina (neutral, 175 mesh) column chromatography using hexane-EtOAc (80:20) as eluent; Yield 66% (78 mg); Reddish yellow liquid;  $R_f$  0.40 (2:1 hexane-EtOAc); IR (KBr) 3059 (=C–H), 2965–2860 (C–H), 1722 (C=O), 1609–1574 (C=C), 1423–1383 (C–H bend), 799 (=C–H bend)  $\text{cm}^{-1}$ ;  $^1\text{H}$  NMR (400 MHz,  $\text{CDCl}_3$ )  $\delta$  8.21–8.14 (m, 2H), 7.75 (d,  $J = 7.5$  Hz, 1H), 7.47 (dd,  $J = 7.8, 7.3$  Hz, 1H), 7.40 (m, 2H), 7.35–7.23 (m, 4H), 7.20 (d,  $J = 7.3$  Hz, 1H), 7.16 (d,  $J = 7.3$  Hz, 1H), 7.14–7.08 (m, 3H), 7.02–6.89 (m, 5H), 5.72 (s, 2H), 5.59 (s, 2H), 4.45 (q,  $J = 7.1$  Hz, 2H), 1.40 (t,  $J = 7.1$  Hz, 3H);  $^{13}\text{C}$  NMR (100 MHz,  $\text{CDCl}_3$ )  $\delta$  166.2, 146.5, 145.9, 143.2, 141.7, 138.4, 138.1, 136.9, 135.7, 129.0, 128.2, 128.1, 128.0, 127.8, 126.7, 126.6, 126.4, 123.3, 122.7, 121.2, 121.1, 121.0, 120.9, 120.0, 110.6, 109.6, 105.52, 105.48, 61.8, 47.7, 46.8, 14.4; HRMS (ESI) calcd for  $[\text{C}_{36}\text{H}_{29}\text{N}_3\text{O}_2 + \text{H}^+]$  536.2333, found 536.2349.



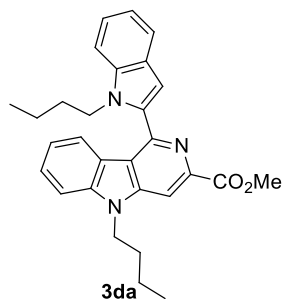
*Tert-butyl 5-benzyl-1-(1-benzyl-1H-indol-2-yl)-5H-pyrido[4,3-b]indole-3-*

*carboxylate (3bc)*. According to the general procedure mentioned above, **1b** (0.100 g, 0.62 mmol), **2c** (52 mg, 0.31 mmol) and DIPEA (0.190 mL, 1.09 mmol) were heated in a sealed tube at 120 °C for 8 h. After workup, crude mixture was purified through alumina (neutral, 175 mesh) column chromatography using hexane-EtOAc (85:15) as eluent; Yield 66% (84 mg); Yellow solid; m.p. = 148–150 °C;  $R_f$  0.60 (2:1 hexane-EtOAc); IR (ATR) 3062 (=C–H), 2926–2848 (C–H), 1706 (C=O), 1665–1531 (C=C), 1495–1323 (C–H bend), 782–694 (=C–H bend)  $\text{cm}^{-1}$ ;  $^1\text{H}$  NMR (400 MHz,  $\text{CDCl}_3$ )  $\delta$  8.28 (d,  $J$  = 8.0 Hz, 1H), 8.06 (s, 1H), 7.75 (d,  $J$  = 7.8 Hz, 1H), 7.47 (dd,  $J$  = 7.5, 7.3 Hz, 1H), 7.43–7.36 (m, 2H), 7.34–7.22 (m, 4H), 7.21–7.15 (m, 2H), 7.15–7.10 (m, 3H), 7.02–6.93 (m, 5H), 5.86 (s, 2H), 5.58 (s, 2H), 1.63 (s, 9H);  $^{13}\text{C}$  NMR (100 MHz,  $\text{CDCl}_3$ )  $\delta$  165.2, 146.4, 146.1, 144.5, 141.7, 138.6, 138.1, 137.0, 135.8, 129.0, 128.2, 128.0, 127.84, 127.75, 126.7, 126.5, 126.4, 123.3, 122.7, 121.2, 121.1, 120.9, 120.4, 120.0, 110.6, 109.6, 105.7, 104.9, 81.8, 47.5, 46.8, 28.2; HRMS (ESI) calcd for  $[\text{C}_{38}\text{H}_{33}\text{N}_3\text{O}_2+\text{H}^+]$  564.2646, found 564.2644.



*Methyl 5-(4-methoxybenzyl)-1-(1-(4-methoxybenzyl)-1H-indol-2-yl)-*

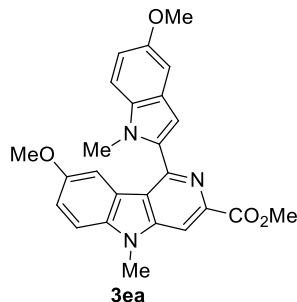
*5H-pyrido[4,3-b]indole-3-carboxylate (3ca)*. According to the general procedure mentioned above, **1c** (0.100 gms, 0.38 mmol), **2a** (24 mg, 0.19 mmol) and DIPEA (0.120 mL, 0.66 mmol) were heated in a sealed tube at 120 °C for 3 h. After workup, crude was purified through alumina (neutral, 175 mesh) column chromatography using hexane-EtOAc (85:15) as eluent; Yield 66% (84 mg); Yellow solid; m.p. = 106–108 °C;  $R_f$  0.60 (2:1 hexane-EtOAc); IR(ATR) 3056 (=C–H), 2952–2835 (C–H), 1737 (C=O), 1664–1512 (C=C), 1457–1348 (C–H bend), 1106–989 (C–O), 819–695 (=C–H bend)  $\text{cm}^{-1}$ ;  $^1\text{H}$  NMR (400 MHz,  $\text{CDCl}_3$ )  $\delta$  8.22 (s, 1H), 8.04 (d,  $J = 8.0$  Hz, 1H), 7.73 (d,  $J = 7.8$  Hz, 1H), 7.51–7.39 (m, 3H), 7.27 (d,  $J = 7.3$  Hz, 1H), 7.18 (dd,  $J = 7.5, 7.0$  Hz, 1H), 7.12 (dd,  $J = 7.3, 7.3$  Hz, 1H), 7.07 (d,  $J = 8.5$  Hz, 2H), 7.06 (s, 1H), 6.85 (d,  $J = 8.8$  Hz, 2H), 6.83 (d,  $J = 8.8$  Hz, 2H), 6.45 (d,  $J = 8.5$  Hz, 2H), 5.55 (s, 2H), 5.54 (s, 2H), 3.99 (s, 3H), 3.76 (s, 3H), 3.52 (s, 3H);  $^{13}\text{C}$  NMR (100 MHz,  $\text{CDCl}_3$ )  $\delta$  166.9, 159.4, 158.4, 146.6, 145.7, 142.9, 141.7, 138.0, 137.0, 130.4, 128.1, 127.95, 127.92, 127.75, 127.68, 123.3, 122.6, 121.2, 121.1, 121.04, 121.01, 119.9, 114.5, 113.5, 110.6, 109.6, 105.7, 105.3, 55.3, 55.1, 52.9, 47.2, 46.4; HRMS (ESI) calcd for  $[\text{C}_{37}\text{H}_{31}\text{N}_3\text{O}_4+\text{H}^+]$  582.2387, found 582.2373.



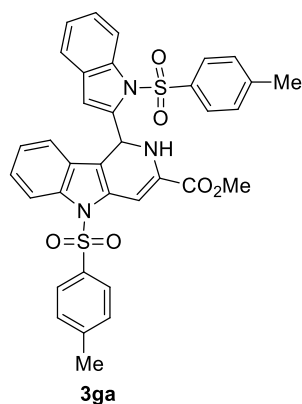
*Methyl 5-butyl-1-(1-butyl-1H-indol-2-yl)-5H-pyrido[4,3-b]indole-3-*

*carboxylate*(**3da**). According to the general procedure mentioned above, **1d** (0.100 g, 0.49 mmol), **2a** (31 mg, 0.25 mmol) and DIPEA (0.114 mL, 0.88 mmol) were heated in a sealed tube at 120 °C for 3 h. After workup, crude was purified through alumina (neutral, 175 mesh) column chromatography using hexane-EtOAc (85:15) as eluent; Yield 66% (84 mg); Yellow liquid;  $R_f$  0.60 (2:1 hexane-EtOAc); IR (KBr) 3064 (=C–H), 2972–2854 (C–H), 1726 (C=O), 1621–1570 (C=C), 1462–1317 (C–H bend), 796 (=C–H bend)  $\text{cm}^{-1}$ ;  $^1\text{H}$  NMR (400 MHz,  $\text{CDCl}_3$ )  $\delta$  8.27 (s, 1H), 8.00 (d,  $J = 8.0$  Hz, 1H), 7.72 (d,  $J = 7.5$  Hz, 1H), 7.59–7.45 (m, 3H), 7.30 (dd,  $J = 7.6, 7.5$  Hz, 1H), 7.18 (dd,  $J = 8.2, 7.2$  Hz, 1H), 7.13 (dd,  $J = 8.2, 7.3$  Hz, 1H), 6.97 (s, 1H), 4.43 (t,  $J = 6.8$  Hz, 2H), 4.34 (t,  $J = 7.0$  Hz, 2H), 4.05 (s, 3H), 2.00–1.87 (m, 2H), 1.71–1.60 (m, 2H), 1.52–1.39 (m, 2H), 1.16–1.04 (m, 2H), 0.99 (t,  $J = 7.0$  Hz, 3H), 0.62 (t,  $J = 7.3$  Hz, 3H);  $^{13}\text{C}$  NMR (100 MHz,  $\text{CDCl}_3$ )  $\delta$  167.1, 146.8, 145.4, 142.7, 141.6, 137.7, 136.9, 127.92, 127.87, 123.3, 122.2, 121.3, 120.9, 120.8\*, 119.6, 110.2, 109.3, 105.6, 104.7, 52.9, 43.9, 43.4, 32.2, 31.1, 20.6, 20.0, 13.9, 13.5; HRMS (ESI) calcd for  $[\text{C}_{29}\text{H}_{31}\text{N}_3\text{O}_2+\text{H}^+]$  454.2489, found 454.2559.

\*Carbon merged



*Methyl 8-methoxy-1-(5-methoxy-1-methyl-1H-indol-2-yl)-5-methyl-5H-pyrido[4,3-b]indole-3-carboxylate (3ea).* According to the general procedure mentioned above, **1e** (70 mg, 0.37 mmol), **2a** (23 mg, 0.18 mmol) and DIPEA (0.110 mL, 0.63 mmol) were heated in a sealed tube at 120 °C for 3 h. After workup, crude mixture was purified through alumina (neutral, 175 mesh) column chromatography using hexane-EtOAc (85:15) as eluent; Yield 66% (84 mg); Yellow solid; m.p. = 160–162 °C;  $R_f$  0.60 (2:1 hexane-EtOAc); IR (ATR) 3070 (=C–H), 2957–2850 (C–H), 1701 (C=O), 1660–1528 (C=C), 1485–1329 (C–H bend), 1105–991 (C–O), 810–688 (=C–H bend)  $\text{cm}^{-1}$ ;  $^1\text{H}$  NMR (400 MHz,  $\text{CDCl}_3$ )  $\delta$  8.26 (s, 1H), 7.40 (d,  $J$  = 9.8 Hz, 1H), 7.32 (d,  $J$  = 8.8 Hz, 1H), 7.21–7.16 (m, 2H), 7.15 (d,  $J$  = 2.0 Hz, 1H), 6.97 (dd,  $J$  = 9.0 Hz, 2.3 Hz, 1H), 6.91 (s, 1H), 4.05 (s, 3H), 3.96 (s, 3H), 3.89 (s, 3H), 3.71 (s, 3H), 3.55 (s, 3H);  $^{13}\text{C}$  NMR (100 MHz,  $\text{CDCl}_3$ )  $\delta$  167.0, 154.8, 154.3, 146.3, 145.8, 142.6, 137.9, 137.2, 133.8, 128.1, 121.2, 120.8, 117.7, 112.8, 110.4, 109.9, 105.8, 105.0, 103.8, 102.5, 55.8, 55.7, 53.0, 31.1, 29.6; HRMS (ESI) calcd for  $[\text{C}_{25}\text{H}_{23}\text{N}_3\text{O}_4+\text{H}^+]$  430.1761, found 430.1764.



*Methyl 5-tosyl-1-(1-tosyl-1H-indol-2-yl)-2,5-dihydro-1H-pyrido[4,3-*

*b]indole-3-carboxylate (3ga).* According to the general procedure mentioned above, **1g** (0.100 g, 0.33 mmol), **2a** (21 mg, 0.17 mmol) and DIPEA (0.101 mL, 0.58 mmol) were heated in a sealed tube at 120 °C for 8 h. After workup, crude was purified through alumina (neutral, 175 mesh) column chromatography using hexane-EtOAc (90:10) as eluent; Yield 63% (70 mg); Yellow solid; m.p. = 205–207 °C;  $R_f$  0.60 (2:1 hexane-EtOAc); IR (ATR) 3413 (N–H), 3062 (=C–H), 2956–2850 (C–H), 1706 (C=O), 1633–1489 (C=C), 1448–1350 (C–H bend), 1307 (N–S=O), 1145 (S=O), 812–687 (=C–H bend)  $\text{cm}^{-1}$ ;  $^1\text{H}$  NMR (400 MHz,  $\text{CDCl}_3$ )  $\delta$  8.16 (dd,  $J = 8.0, 8.0$  Hz, 2H), 7.73 (d,  $J = 8.5$  Hz, 2H), 7.70 (d,  $J = 8.5$  Hz, 2H), 7.32–7.26 (m, 3H), 7.24–7.19 (m, 3H), 7.18–7.14 (m, 2H), 7.09 (d,  $J = 2.0$  Hz, 1H), 6.98 (dd,  $J = 7.5, 7.3$  Hz, 1H), 6.59 (d,  $J = 2.0$  Hz, 1H), 6.38 (d,  $J = 7.8$  Hz, 1H), 5.90 (s, 1H), 5.64 (s, 1H), 3.83 (s, 3H), 2.41 (s, 3H), 2.37 (s, 3H);  $^{13}\text{C}$  NMR (100 MHz,  $\text{CDCl}_3$ )  $\delta$  163.9, 145.4, 145.0, 139.4, 137.7, 137.4, 136.3, 135.2, 135.0, 132.6, 130.1, 129.9, 128.8, 127.7, 126.8, 126.3, 125.2, 124.4, 124.0, 123.8, 121.2, 117.5, 114.9, 114.8, 113.1, 110.6, 94.4, 52.6, 47.9, 21.7, 21.6; HRMS\* (ESI) calcdfor[ $\text{C}_{35}\text{H}_{27}\text{N}_3\text{O}_6\text{S}_2+\text{H}^+$ ] 650.1414, found 650.1386.

\*HRMS peak corresponds to dehydrogenated (aromatized) form of **3ga**.

## 4.2. *In vitro* cytotoxicity studies

### 4.2.1. *Cytotoxicity analysis in cancer and macrophage cells*

Cancer (MCF7, A431, A549, HEK293 or HeLa cell lines) or RAW264.7 cells were seeded in a 96 well plate (4,200 cells/well) and allowed to form a monolayer for a period of 48 h. Old medium was replaced with fresh medium (0.2 mL) containing an increasing concentration of  $\gamma$ -carboline derivatives **3ac**, **3bc**, **3ca** and **3ga** (0.1  $\mu$ M, 0.25  $\mu$ M, 0.5  $\mu$ M, 1  $\mu$ M, 2.5  $\mu$ M, 5  $\mu$ M, 10  $\mu$ M, 25  $\mu$ M, 50  $\mu$ M, 100  $\mu$ M) and incubated for 48 h or 3 h, respectively. Spent medium in each well were discarded and cells were rinsed with PBS (3  $\times$  0.2 mL) followed by treatment with 0.5% crystal violet (0.05 mL) for 20 minutes at room temperature. Cells were rinsed with PBS (3  $\times$  0.2 mL), methanol (0.20 mL) was added to each well and incubated for 20 minutes. The absorbance from each well proportional to the live cell was measured using Synergy H1 multimode plate reader (BioTek Instruments, Inc., Winooski, VT, USA) at an excitation and emission wavelength of 530 nm and 590 nm respectively.

Dose vs response curves were obtained from a plot of semi-log[conc] vs intensity of fluorescence emission and IC<sub>50</sub> (concentration at which 50% of the enzymatic activity is inhibited) was calculated for carboline derivative using GraphPad Prism, version 7.02 for Windows (GraphPad Software, San Diego, CA).

### 4.2.2. *HeLa cell uptake study of $\gamma$ -carboline 3ac*

Live cell imaging experiment was performed on HeLa cells. HeLa cells were plated in a 4-well confocal dish (cell count  $\sim$ 100 cells per well) and incubated for 48 h at 37 °C under 5% CO<sub>2</sub>.

After 3 h of incubation with carboline derivative **3ac** (10 nM, 100 nM, 1  $\mu$ M, 10  $\mu$ M, and 100  $\mu$ M), cellular uptake and distribution were monitored by using confocal microscopy ( $\lambda_{\text{ex}} = 405$  nm;  $\lambda_{\text{emrange}} = 420\text{--}470$  nm).

### Declaration of Competing Interest

There are no conflicts of interest to declare.

### Acknowledgements

We would like to extend our sincere gratitude to Sophisticated Instrumentation Centre, Indian Institute of Technology Indore for providing characterization facilities. PD thanks Council for Scientific and Industrial Research, New Delhi for senior research fellowship. MAK and KY thank IIT Indore for research fellowships.

### Appendix A. Supplementary material

Supplementary data to this article can be found online. Copies of  $^1\text{H}$ ,  $^{13}\text{C}$  NMR spectra of **1a–h**, **3aa–3ac**, **3ba–3bc**, **3da**, **3ea**, **3ga**, **12a–b**, **12e–f**, **12i**, **14d**, **14g** and **15**, UV calibration curves in different organic solvents for  $\gamma$ -carboline **3ac**, single crystal XRD data of **3ac** and details for DFT calculations.

### References

1. Reniers, J.; Robert, S.; Frederick, R.; Masereel, B.; Vincent, S.; Wouters, J. *Bioorg. Med. Chem.* **2011**, *19*, 134–144.

2. (a) Alekseyev, R. S.; Kurkin, A. V.; Yurovskaya, M. A. *Chem. Heterocycl. Comp.* **2009**, *45*, 889–925. (b) Pontecorvo, M. J.; Devoussr, M. D.; Navitsky, M.; Lu, M.; Salloway, S.; Schaerf, F. W.; Jennings, D.; Arora, A. K.; McGeehan, A.; Lim, N. C.; Xiong, H.; Joshi, A. D.; Siderowf, A.; Mintun M. A. *BRAIN* **2017**, *140*, 748–763. (c) Snyder, J. K.; Wei, W. G.; Strosberg, A. D.; Kota, S.; Takahashi, V. Small Molecule Inhibitors of Hepatitis C Virus. International Patent WO 2011/056630 A2, October 27, 2010. (d) Guerquin-Kern, J. L.; Coppey, M.; Carrez, D.; Brunet, A. C.; Nguyen, C. H.; Rivalle, C.; Slodzian, G.; Croisy, A. *Micros. Res. Tech.* **1997**, *36*, 287–295. (e) Ran, X.; Zhao, Y.; Liu, L.; Bai, L.; Yang, C. Y.; Zhou, B.; Meagher, J. L.; Chinnaswamy, K.; Stuckey, J. A.; Wang, S. *J. Med. Chem.* **2015**, *58*, 4927–4939.
3. Ibrahim, S. R. M.; Mohamed G. A.; Zayed M. F.; Sayed H. M. *Drug Res.* **2015**, *65*, 361–365.
4. Naik, P. N.; Khan, A.; Kusurkar, R. S. *Tetrahedron* **2013**, *69*, 10733–10738.
5. Jia, T.; Wang, J.; Guo, P.; Yu, J. *Org. Biomol. Chem.* **2015**, *13*, 1234–1242.
6. Otto, R.; Penzis, R.; Gaube, F.; Winckler, T.; Appenroth, D.; Fleck, C.; Tränkle, C.; Lehmann, J.; Enzensperger, C. *Eur. J. Med. Chem.* **2014**, *87*, 63–70.
7. Toure, B. B.; Hall, D. G. *Chem. Rev.* **2009**, *109*, 4439–4486.
8. Tietze, L. F.; Rackelmann, N. *Pure Appl. Chem.* **2004**, *76*, 1967–1983.
9. Tietze, L. F.; Modi, A. *Med. Res. Rev.* **2000**, *20*, 304–322.
10. Nicolaou, K. C.; Edmonds, D. J.; Bulger, P. G. *Angew. Chem., Int. Ed.* **2006**, *45*, 7134–7186.
11. Dai, J.; Dan, W.; Zhang, Y.; Wang, J. *Eur. J. Med. Chem.* **2018**, *157*, 447–461.

12. Alekseev, R. S.; Kurkin, A. V.; Yurovskaya, M. A. *Chem. Heterocycl. Comp.* **2012**, *48*, 1235–1250.
13. Herbert, C. A.; Plattner, J. J.; Welch, W. M.; Weissman, A.; Koe, B. K. *J. Med. Chem.* **1980**, *23*, 635–643.
14. Butler, K. V.; Kalin, J.; Brochier, C.; Vistoli, G.; Langley, B.; Kozikowski, A. P. *J. Am. Chem. Soc.* **2010**, *132*, 10842–10846.
15. Zhang, H.; Larock, R. C. *Tetrahedron Lett.* **2002**, *43*, 1359–1362.
16. Subba Reddy, B. V.; Swain, M.; Reddy, S. M.; Yadav, J. S.; Sridhar, B. *J. Org. Chem.* **2012**, *77*, 11355–11361.
17. Nissen, F.; Richard, V.; Alayrac, C.; Witulski, B. *Chem. Commun.* **2011**, *47*, 6656–6658.
18. Wang, T. T.; Zhang, D.; Liao, W. W. *Chem. Commun.* **2018**, *54*, 2048–2051.
19. Gutiérrez, S.; Sucunza, D.; Vaquero, J. J. *J. Org. Chem.* **2018**, *83*, 6623–6632.
20. Chepyshev, S. V.; Lujan-Montelongo, J. A.; Chao, A.; Fleming, F. F. *Angew. Chem., Int. Ed.* **2017**, *56*, 4310–4313.
21. Hao, W. J.; Wang, S. Y.; Ji, S. J. *ACS Catal.* **2013**, *3*, 2501–2504.
22. Lee, Y.; Klausen, R. S.; Jacobsen, E. N. *Org. Lett.* **2011**, *13*, 5564–5567.
23. Martin, S. F. *Pure Appl. Chem.* **2009**, *81*, 195–204.
24. López-Pérez, A.; Adrio, J.; Carretero, J. C. *Angew. Chem. Int. Ed.* **2009**, *48*, 340–343.
25. Dudhe, P.; Venkatasubbaiah, K.; Pathak, B.; Chelvam, V. *Org. Biomol. Chem.* **2020**, *18*, 1582–1587.
26. Das, T.; Kayet, A.; Mishra, R.; Singh, V. K. *Chem. Commun.* **2016**, *52*, 11231–11234.
27. (a) Frisch, M. J. ; Trucks, G. W.; Schlegel, H. B.; et al., Gaussian 09, Revision D.01, Gaussian, Inc., Wallingford, CT, **2009**. (b) Becke, A. D. *Phys. Rev. A* **1988**, *38*,

3098–3100. (c) Lee, C.; Yang, W.; Parr, R. G. *Phys. Rev. B: Condens. Matter Phys.* **1988**, *37*, 785–789.

28. Zhao, G. J.; Liu, J. Y.; Zhou, L. C.; Han, K. L. *J. Phys. Chem. B* **2007**, *111*, 8940–8945.